Cardiovascular Radiology

Reto A. Meuli, MD • Van J. Wedeen, MD • Stuart C. Geller, MD • Robert R. Edelman, MD
• Lawrence R. Frank, BS • Thomas J. Brady, MD • Bruce R. Rosen, MD, PhD

MR Gated Subtraction Angiography: Evaluation of Lower Extremities[1]

We report the first clinical experience with a new method for projective imaging of blood vessels (angiography) using magnetic resonance. Vascular contrast is produced noninvasively by the phase response of moving protons. Diastolic and systolic gated images produce, respectively, flow signal and flow void; the difference image is a map of the pulsatile flow: an arteriogram. Preliminary studies are presented of the lower extremities of one healthy volunteer and four patients (one each with occlusive disease, soft-tissue tumor, arteriovenous malformation, and venous femoral-popliteal graft). Patient data are compared with accompanying conventional arteriograms, and the new method is discussed.

ROENTGEN angiography and Doppler ultrasonography are the two most frequently used imaging modalities in the assessment of arterial disease. Angiography, although invasive, provides high-resolution anatomic description, while ultrasound provides more functional information. However, both techniques have well-known limitations (1, 2). A noninvasive technique that provides both high-resolution images and functional information about blood flow would be of great value for patients with arterial disease.

The early work of Hahn, Carr, and Purcell demonstrates the effect of flow on magnetic resonance (MR) spin-echo signals (3, 4). With the development of MR imaging, several methods to measure and display blood flow have been introduced (5–10). Like roentgen angiography, conventional MR images provide anatomic assessment of blood vessels, and like Doppler ultrasonography, the MR signal contains physiologic information such as flow velocity. Some clinical work on the assessment of the vascular system by MR already exists (11–17); however, imaging of the body with a section-selective technique is not optimal for the study of the vascular tree. The tortuous anatomy of the arteries frequently prevents a sufficiently long portion of the vessel from appearing in one imaging plane. While three-dimensional reconstruction of vessels is possible (18), the acquisition of MR images in the projective format, like x-ray angiography, provides a direct and useful representation of the vascular structures.

The physical basis and technical principles of MR imaging of blood flow have been presented (5–8) and reviewed (9, 10). Proton motion through the MR imaging gradients creates an endogenous flow-dependent contrast because of its distinctive spin-phase properties. With this contrast, the projective format enables the representation of the three-dimensional vascular tree in a two-dimensional picture, as in a classic x-ray contrast-enhanced angiogram. We have previously reported that subtraction of a systolic from a diastolic projective image cancels the signal from static background protons and leaves only the pulsatile arteries in the image (10). We now present preliminary clinical applications of this noninvasive method of pulsatile blood flow MR imaging in the projective format. Several cases of arterial disease of the lower extremity illustrate the various possibilities of this technique. A discussion of the advantages and limitations is provided.

THEORY

The effects of flow in the current context are presented in reference 10; we present here a synopsis. Our theoretical description centers on the two aspects of our experiments: the projective format (19) and flow-velocity encoding. In conventional MR imaging, section selection is achieved by applying a field gradient perpendicular to the selected plane (z-gradient) during the radio frequency (RF) pulses. When this gradient is left off, however, the RF pulses will excite all the protons contained in the RF coil. Then, as usual, frequency and phase-encoding gradients can be applied along the two other directions (x-axis and y-axis, respectively) to generate an image. With the x-direction parallel to the long axis of the legs, the y-direction mediolateral, and the z-direction anteroposterior, the result is an infinitely thick image, thicker than the legs in the present application.

Motion of excited spins through magnetic gradients results in a phase shift for the spins and the signals detected from them (3, 4). Detailed

analysis of imaging experiments shows that it is primarily the imaging readout gradient that causes detectable velocity-encoding phase shifts in MR image data, at least for the odd-numbered echoes (6–8). For the simplest case, that of an unpulsed readout gradient, the size of the velocity-dependent phase shift, ϕ, is given by the relationship of Carr, Purcell, and Hahn:

$$\phi = \tfrac{1}{4}\langle \gamma G, V \rangle\, t_e{}^2, \tag{1}$$

where γG is the image readout gradient in hertz per centimeter, V is the proton velocity, t_e is the total echo time, and $\langle , \rangle$ denotes the scalar product. To illustrate the idea of velocity sensitivity, suppose that a particular experiment has a velocity sensitivity of 2 cycles/(m sec^{-1}); then protons moving at 1.0 m sec^{-1} will get a 720° phase shift, while protons moving at 5 cm sec^{-1} would be shifted only 36°.

The difference between systolic and diastolic flow velocities and consequent difference in velocity-dependent phase shift is essential for the generation of the contrast using our technique. In the normal superficial femoral artery, the peak systolic velocity is between 0.5 and 1 m sec^{-1}, while in end diastole the flow is practically zero (20). With a projective format, a voxel crossing a vessel is like a long tube containing mainly static protons and a relatively small amount of moving protons. During diastole the signal arising from the static protons and from the slow-moving blood behaves coherently. This gives a maximal signal intensity of the voxel through the vessel. During systole the flowing protons present a

distribution of phase corresponding to the distribution in velocities across the vessel. This causes the signal arising from the blood protons to cancel, and thus a loss of signal from voxels intersecting the vessel will result. A subtraction of the systolic from the diastolic image removes all the static background and leaves only the arteries and background noise in the image.

The visibility of a vessel with this technique depends on both its flow characteristics and its orientation. Vessels with flow that is insufficiently pulsatile, with diastolic velocities too high, or with systolic velocities too low will exhibit little or no
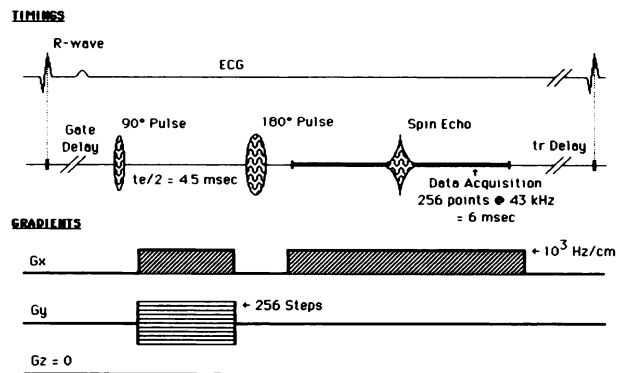

Figure 1. Conventional ECG-gated two-dimensional Fourier transform spin-echo pulse sequence used for these studies. See text for complete description. (Adapted and reprinted, with permission, from [10].)
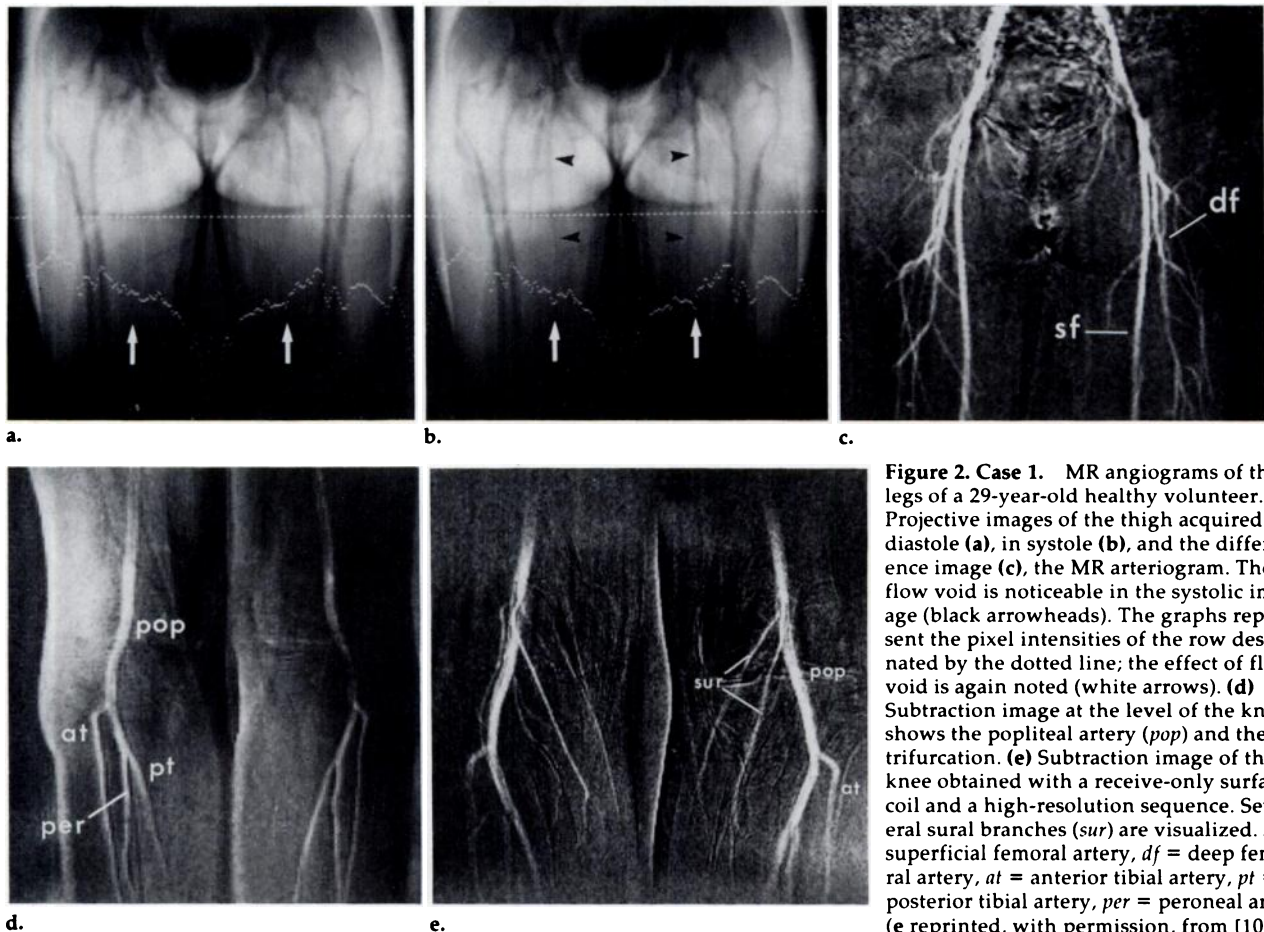

Figure 2. Case 1. MR angiograms of the legs of a 29-year-old healthy volunteer. Projective images of the thigh acquired in diastole (a), in systole (b), and the difference image (c), the MR arteriogram. The flow void is noticeable in the systolic image (black arrowheads). The graphs represent the pixel intensities of the row designated by the dotted line; the effect of flow void is again noted (white arrows). (d) Subtraction image at the level of the knee shows the popliteal artery (pop) and the trifurcation. (e) Subtraction image of the knee obtained with a receive-only surface coil and a high-resolution sequence. Several sural branches (sur) are visualized. sf = superficial femoral artery, df = deep femoral artery, at = anterior tibial artery, pt = posterior tibial artery, per = peroneal artery. (e reprinted, with permission, from [10].)

contrast. As a result, venous structures are usually invisible. In addition, contrast is influenced by the component of the flow velocity vectors parallel to the readout gradient, not by the absolute speed of flow. A vessel that shows good contrast when oriented parallel to the readout gradient may lose contrast if the image is reoriented so that the vessel is oblique; in the extreme case of a vessel perpendicular to the readout coordinate, there will be no contrast at all. We shall return to these points in the Discussion.

METHODS

Imaging was performed with a commercial 0.6-T (25-MHz, proton) superconducting imaging system (Technicare, Solon, Ohio) using modifications of the currently available software. Our pulse sequence is presented in Figure 1. The 90° and 180° pulses are broadband (<500 μsec), square-shaped pulses. The image axes are oriented for a frontal projection. Velocity sensitivity must be of such size as to cause small phase shifts (≤ 0.1 cycle) for protons moving at diastolic velocities (0–5 cm sec^{-1}) and large ones (≥ 1 cycle) for systolic velocities (about 1 m sec^{-1}). Two imaging pulse sequences were constructed to meet these requirements. The first, for use with the 50-cm body coil, uses a readout gradient of 1 kHz cm^{-1} and a data acquisition period of 6 msec sampled at 43.5 kHz to give a spatial resolution of 1.8 mm. With an echo time of 11 msec, it has a velocity sensitivity of 1.5 cycles/(m sec^{-1}) (phase shift per velocity). The second pulse sequence is used with a square 30-cm surface coil. The sampling period is lengthened to 8.5 msec (and the sampling rate reduced proportionally) for an improved spatial resolution, 1.2 mm. The echo time is increased to 14 msec, raising the velocity sensitivity to 2.5 cycles/(m sec^{-1}).

Data acquisition is synchronized with the electrocardiogram (ECG). Gated imaging is accomplished with a manufacturer-supplied interface to a Hewlett-Packard ECG radio telemetry device. Diastolic flow is regularly detected by imaging with a gate delay of 5 msec from the R wave. The arrival time of peak systolic flow is variable. In healthy individuals, the arrival time increases predictably with distance from the heart. Arterial disease may either retard the pulse wave (e.g., in cases of aneurysm or occlusion) or accelerate it (e.g., in cases of nonocclusive atherosclerosis) (21). Two methods of selecting an appropriate systolic gate delay have been used. One approach is to acquire three or four low-resolution angiographic images to explore the range of plausible systolic gate delays in 50-msec increments. With acquisitions of 128 phase-encoding steps and one signal average, these require 128 heartbeats or about 2 minutes each. Each candidate systolic image is subtracted in turn from the same diastolic "mask," so that a total of about five images are needed, requiring about 15 minutes to obtain. Alternatively, ECG and Doppler flow tracings may be recorded concurrently and compared for direct determination of the temporal relation between peak flow and the QRS complex. In both cases, a determination is made at a single location, and delays appropriate to proximal and distal sites are estimated; we add about 50 msec for each linear foot from the heart.

When a satisfactory systolic gate delay is found, imaging is repeated with high resolution. Each image uses 256 phase-encoding steps and two signal averages; at two image acquisitions per study, each MR arteriogram requires 1,024 heartbeats or about 15 minutes. Magnitude images are displayed and subtracted without the use of frame shifting techniques. Images of patients with lower limb arterial diseases are correlated with x-ray angiograms.
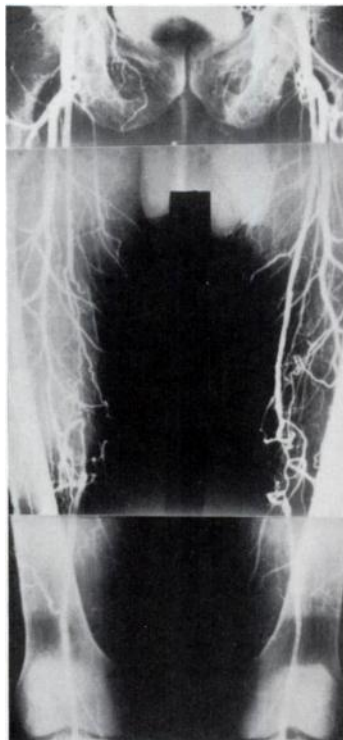
RESULTS

Case 1.—The first subject is a 29-year-old female volunteer with no clinical history of cardiovascular disease. Figure 2a and 2b present magnitude images of the thigh acquired in systole and diastole. The flow void caused by the fast-flowing blood is noticeable in the major vessels in the systolic image. The result of the subtraction of the systolic from the diastolic image is presented in Figure 2c. The background is almost completely canceled, and the common femoral, superficial femoral, and deep femoral arteries with their several branches are clearly visualized. Figure 2d shows the subtraction image in the same subject at the level of the popliteal arteries and the tibial trifurcation. Figure 2e is a higher-resolution surface coil image of the same area, allowing visualization of two small sural branches on either side. The x-ray angiogram is unavailable for correlation with these images.

Case 2.—This patient is a 60-year-old man with a 1-year history of bilateral claudication. X-ray angiographic examination demonstrated focal stenosis of both iliac arteries and a segmental obstruction of both superficial femoral arteries. A dilatation of the iliac stenosis was performed. After this procedure, MR angiography of the thigh was also performed. The resulting image and the postdilatation x-ray angiogram are presented in Figure 3a and 3b. The x-ray angiogram shows the system of collateral arteries arising from the right deep femoral artery. Collaterals are also present on the left side but arise mostly from the proximal segment of the superficial femoral artery. On the MR image both common and deep femoral arteries are clearly visualized. The system of collaterals on the right is also noticeable. The contrast is well preserved in both popliteal arteries in spite of the superficial femoral obstruction. Finally, we note no contrast from the proximal segment of the right superficial femoral artery, a segment evidently open as shown on the radiograph. This point will be discussed later.
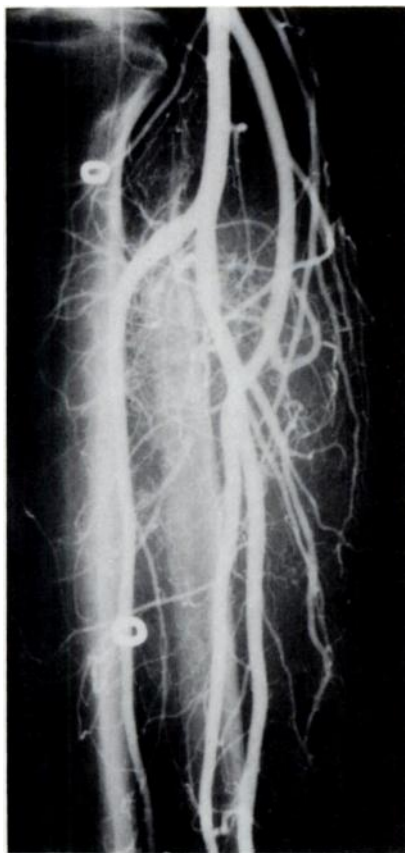
Case 3.—The third subject is a 38-year-old man who presented with a soft-tissue mass (lymphangioma) in the left calf. A frontal and a lateral view of the x-ray angiogram of the left calf are presented in Figure 4a and 4b. The MR angiogram obtained with a surface coil positioned posteriorly is presented in Figure 4c. The origin of the left posterior tibial artery is visualized less clearly on the MR image than it is on the x-ray image because of the slightly different projections. The low contrast of the anterior tibial artery is caused by its greater distance from the surface of the receiver coil. In contradistinction, the sural branches located posteriorly close to the coil show excellent contrast. The smallest segments of these arteries shown by the MR image are about 1 mm in diameter.

Case 4.—This patient is a 22-year-old man with extensive arteriovenous malformations (AVMs) in the left leg. Digital x-ray angiograms of the thigh and the calf are presented in Figure 5a and 5b. Figure 5a is a superposition of the arterial and venous phase; Figure 5b shows only the arterial phase. Figure 5c and 5d show the MR study in the thigh and calf. The
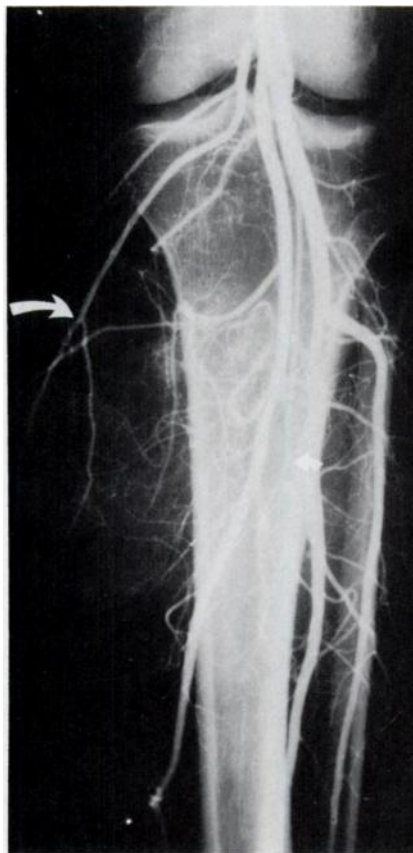
Figure 4. Case 3. Images of a 38-year-old man with a soft-tissue mass (lymphangioma) in the left calf. Arteriograms, lateral (a) and anteroposterior (b) projections. (c) MR angiogram, anteroposterior projection. The patient has an anterior tibial-peroneal trunk and a separate high origin of the posterior tibial artery from the popliteal artery (*pop*) at the level of the knee joint. The position of the limb is not exactly the same in b and c, resulting in superimposition in c of the proximal posterior tibial artery with the anterior tibial-peroneal trunk. Therefore the origin of the posterior tibial artery is not visualized in c. The sural arteries show good contrast in c because they are close to the receiver surface coil. White arrows show the correspondence in sural branches in b and c. *per* = peroneal artery, *at* = anterior tibial artery, *pt* = posterior tibial artery. ▼
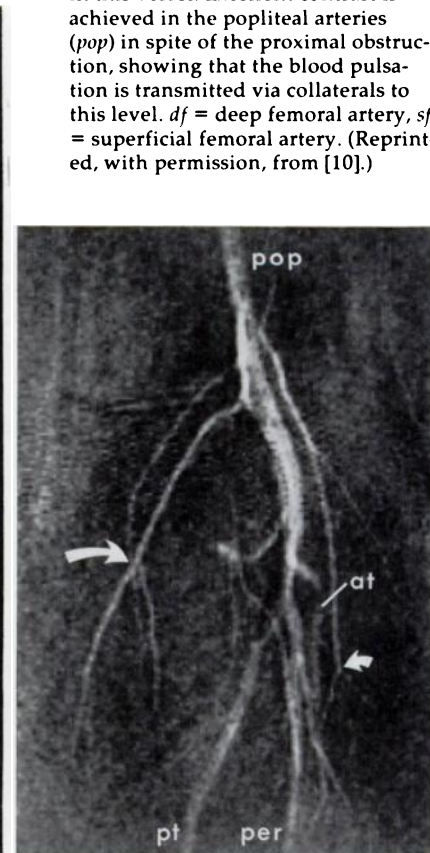
b.

a.

Figure 3. Case 2. Images of a 60-year-old-man with bilateral obstruction of the superficial femoral artery. (a) Conventional arteriogram shows obstructions on both superficial femoral arteries. (b) MR angiogram of the thighs. The proximal segment of the right superficial femoral artery is not visualized because of the poor runoff in this vessel. Excellent contrast is achieved in the popliteal arteries (*pop*) in spite of the proximal obstruction, showing that the blood pulsation is transmitted via collaterals to this level. *df* = deep femoral artery, *sf* = superficial femoral artery. (Reprinted, with permission, from [10].)
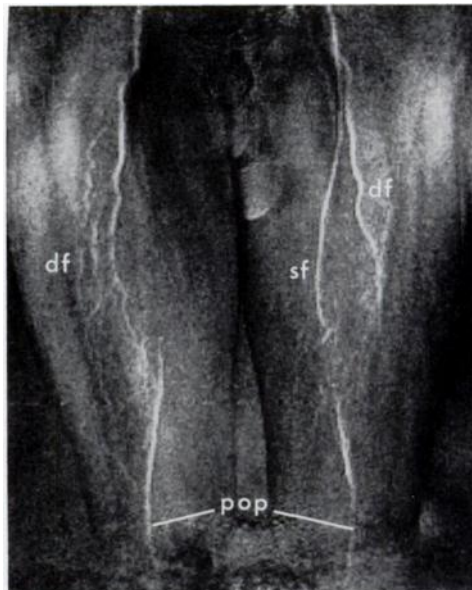
a.

b.

c.

superficial femoral, the popliteal, and the origin of the anterior tibial arteries are normally visualized in the MR image of the right thigh. The left leg shows a severe arterial abnormality in this patient; the nor-

mal blood pulsation (as demonstrated by Doppler ultrasound) is completely disturbed by the abnormal vascular system of the left leg. The large-caliber vessels leading to the AVM reduce the normal time lag
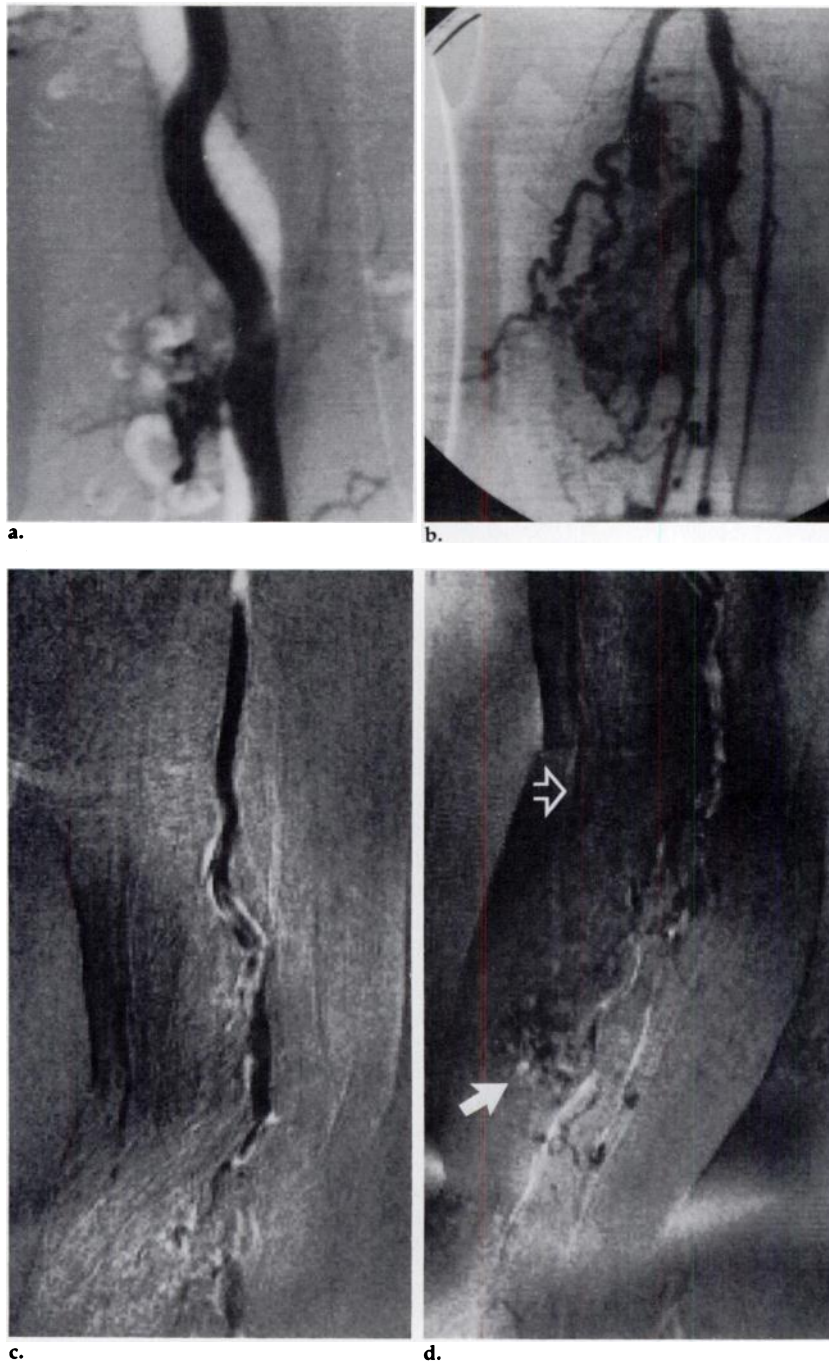
Figure 5. Case 4. Images of a 22-year-old man with AVMs in the left leg. (a) X-ray digital subtraction angiogram (DSA) of the left thigh shows the superficial femoral artery in black and the femoral veins in white. (b) DSA of the left calf shows the arterial contrast phase with AVM. (c, d) MR angiograms show the superficial femoral artery and the abnormal vascular system of the calf. Closed white arrow shows an AVM area. The blood pulsation is transmitted through this AVM and generates a contrast in a superficial vein (open arrow). Arteries of the right legs are normally visualized in c.

between central and peripheral pulsation. In the MR image, this results in reversal of the contrast in the femoral and popliteal arteries after subtraction of the "systolic" from the "diastolic" image. Pulsatility in terminal vessels of the AVM is complex, resulting in a mixture of black and white within the AVM. Two regions of AVM are depicted by MR; correlation with the x-ray angiogram is good. In the thigh MR shows only the superficial femoral artery and not the femoral veins, as shown by a comparison of Figure 5a and 5c. In the calf, the blood pulsation is transmitted through the AVM to generate contrast in the superficial veins (Fig. 5d).

Case 5.—This patient is a 73-year-old man with a history of claudication in the left leg. An x-ray angiogram (Fig. 6a) shows an almost complete occlusion of the left superficial femoral artery with a good

runoff below the knee. An MR study was then performed, which correlated well with x-ray angiography (Fig. 5b). A left femoral popliteal graft was performed. Fourteen days after surgery, an MR study with a surface coil was performed to visualize the distal anastomosis (Fig. 6c). The contrast achieved in both MR images is low compared with the other results presented in this work. This case is presented to show how our methods work with an elderly patient having low cardiac output and small arteries with arteriosclerotic disease at several levels. Misregistration caused by patient motion also affects the image quality. However, the distal portion of the graft and the anastomoses are visualized and prove the patency of the graft. Finally, the proximal segment of the left superficial femoral artery is poorly visualized by MR, as in case 2.
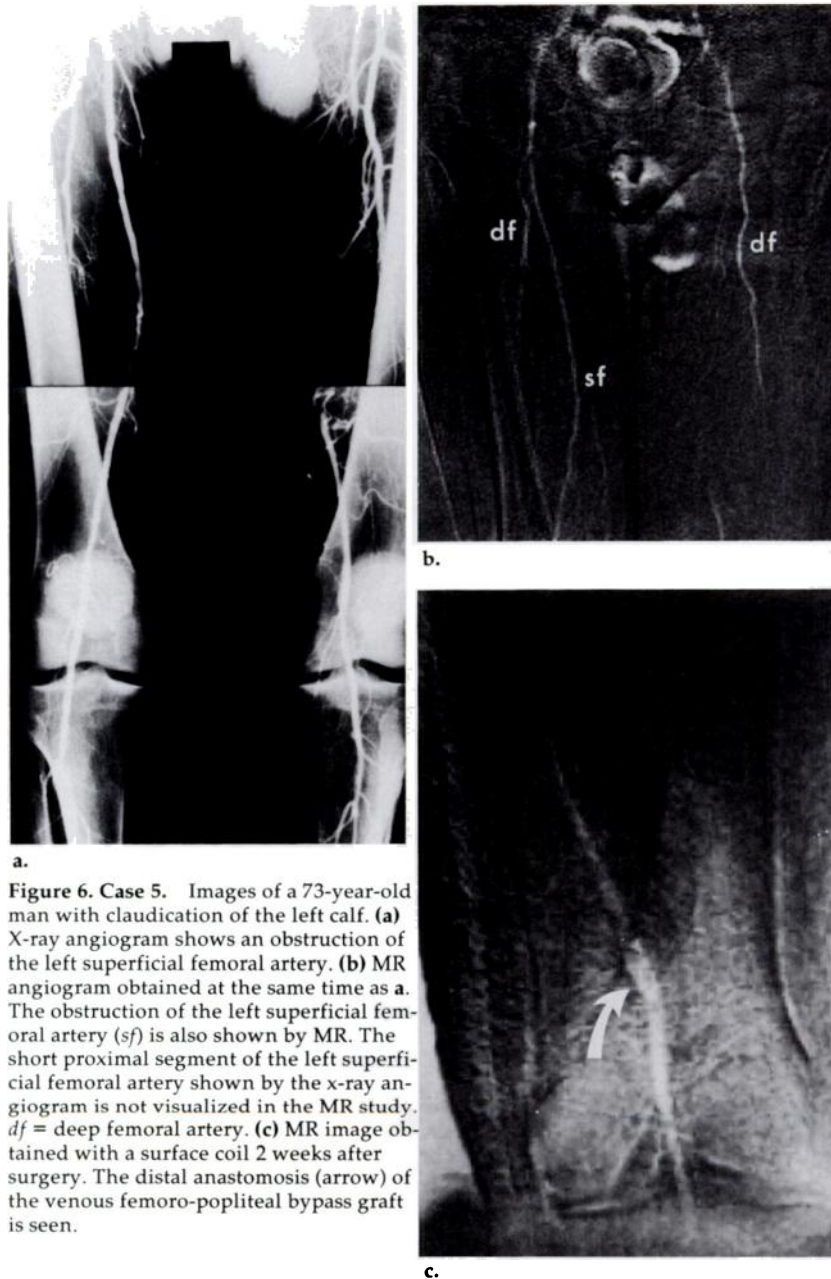
Figure 6. Case 5. Images of a 73-year-old man with claudication of the left calf. **(a)** X-ray angiogram shows an obstruction of the left superficial femoral artery. **(b)** MR angiogram obtained at the same time as **a**. The obstruction of the left superficial femoral artery (*sf*) is also shown by MR. The short proximal segment of the left superficial femoral artery shown by the x-ray angiogram is not visualized in the MR study. *df* = deep femoral artery. **(c)** MR image obtained with a surface coil 2 weeks after surgery. The distal anastomosis (arrow) of the venous femoro-popliteal bypass graft is seen.

DISCUSSION

These preliminary data demonstrate that MR imaging angiograms of intermediate resolution can be obtained in healthy people and in patients with diverse vascular disorders. The MR imaging data correlated well with state-of-the art contrast arteriograms when the latter were available. Unlike conventional angiography, the method we describe is noninvasive, requiring no catheterization or injection of contrast agent. Compared with Doppler ultrasonography, the one preexisting method for noninvasive vascular imaging, MR angiography is not a real-time method, but it has a wide field of view, is operator independent, and has the potential to assess any area in the body. The resemblance of these images to conventional angiograms disguises a wealth of difference. This difference results from universal characteristics of MR imaging (e.g., its spatial resolu-

tion, its non-real-time character, and its typical artifacts) and from the distinctive properties of the flow contrast we have demonstrated (e.g., its directional sensitivity and dependence on pulsatility). This distinction should be kept in mind when, in the following critical discussion, we suggest several ways to refine and extend the current method.

Sensitivity of the contrast to the direction of flow is a basic feature of the current method and stems directly from the nature of velocity-phase encoding. In the setting of quantitative flow imaging, this sensitivity generates much useful information (7). In the current setting (imaging for arterial morphology), however, the directional dependence of the flow contrast is an inconvenience. If the vessels of interest were randomly oriented in three dimensions, it would be necessary to obtain three MR angiograms, one sensitive to flow along each of the three coordinate axes, and combine the results. We believe that this procedure is often superfluous in the human ex-
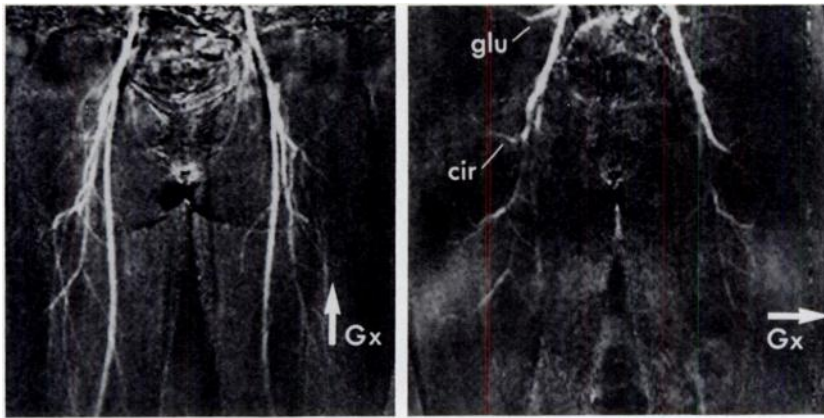
a.   b.

Figure 7. Views of the legs of a healthy volunteer demonstrate the dependence of flow contrast on the orientation of the image gradients. **(a)** The image x-gradient is vertical (G_x); superficial and deep femoral systems are seen. **(b)** The x-gradient is rotated clockwise 90° (is horizontal, G_x); contrast is improved in the lateral femoral circumflex (*cir*) and the inferior gluteal (*glu*) arteries but is nearly eliminated in the superficial and deep femoral systems.

tremities because the vascular anatomy is highly directional, parallel to the axes of the limbs. This idea was tested in healthy people; Figure 7 shows typical data. Two angiograms were acquired under identical conditions except that the x and y image coordinates were interchanged. The angiogram acquired with the readout gradient Gx (the flow sensitivity) in the preferred axial orientation shows the superficial and deep femoral systems. The image acquired with the readout gradient reoriented in the horizontal direction contributes little to the image of the femoral arteries, but it does demonstrate the more horizontal superior gluteal and lateral femoral circumflex arteries. This suggests that acquisition of two or more views with perpendicular velocity sensitivities will probably be appropriate in the abdomen and pelvis.

As stated earlier, vascular contrast results only when two independent conditions are met: a diastolic flow velocity sufficiently low that blood signal is preserved and a systolic flow sufficiently rapid that blood signal is ablated. The fact that there are two requirements for contrast rather than just one can complicate image interpretation. Consider, for example, case 2. Figure 3b demonstrates that the popliteal arteries are patent and pulsatile bilaterally, supplied by unseen collaterals. Yet it is in doubt precisely why the collaterals are invisible. The small size of these vessels is an obvious factor, but their flow physiology must also be considered; because they are narrow, they may have an elevated diastolic flow velocity and so yield low contrast. However, it would also be consistent to postulate that the collaterals had an enlarged aggregate cross section, and so the systolic velocities are too low for good contrast. This interpretive dilemma is likely to recur in the setting of focal stenosis, which elevates diastolic velocities and possibly reduces systolic velocities as well (21).

A related difficulty of the present method is the need to determine an appropriate systolic gate delay. Preliminary data indicate that the current method is tolerant of changes in the gate delay smaller than 50 msec, and that reduced contrast, when it occurs, will be noted first in the small branch vessels 1–2 mm in diameter. We have suggested three approaches to

this problem: scout films, Doppler measurement, and estimation. However, it is not yet clear which of these is most efficient.

Though sensitivity to blood pulsation is not without interest, there is a wide gap between the view of the vascular system provided by this form of contrast and the familiar, more anatomic view provided by conventional x-ray contrast-enhanced imaging. A new method under development aims to bridge this gap. In brief, one creates two pulse sequences, one sensitive to flow and the other totally insensitive to flow, and subtracts the images that result. (The flow-insensitive pulse sequence might be an even-echo experiment [22].) The flow-insensitive acquisition plays the role of a diastolic acquisition, depicting the blood in all cases. The flow-sensitive acquisition serves as a systolic acquisition: It will show a flow void wherever blood moves faster than some threshold value. We have named this method "heterogeneous subtraction." Note that the velocity sensitivity of the flow-sensitive image can be freely adjusted, technique permitting, without injuring the ability of its companion image to record a blood signal. As a result, this revised method would extend contrast to slow flow or continuous, nonpulsatile flow (e.g., venous flow) and could operate in either a gated or an ungated mode.

Two minor artifacts endemic to Fourier transform flow imaging deserve comment. First, because position encoding is not simultaneous in x and y, a vessel flowing at an oblique angle to the image coordinates will appear displaced a small distance at a right angle to its axis. The size of this displacement depends on the length of time between the center of the phase-encoding pulse and the center of the spin echo, and on the diastolic flow velocity (blood signal is detected only in the diastolic image) (6, 23). For example, if the diastolic velocity is 10 cm sec^{-1} and the named time interval is 10 msec, then an apparent displacement of ≤ 1 mm could result. Second, blood adjacent to the vessel wall will move slowly even in systole and so may give rise to a detectable signal. This will undercut the flow contrast and cause the image of the vessel to have an artifactually small diameter.

It has been suggested that changes of arterial position, diameter, and volume with the pulse could be independent sources of image artifact, perhaps by causing a misregistration between systolic and diastolic images. We believe that this is not the case on the following grounds: Because there is little contrast between the blood and its surroundings in the diastolic image (far less than the contrast between the vessel wall and the flow void of the systolic), the contour of the blood-filled diastolic vessel is unimportant. In other terms, it is the systolic image that contains the main share of the vascular information. This view, if correct, has an interesting corollary: A diastolic image of reduced spatial resolution would make an adequate mask for image subtraction. The use of a low-resolution diastolic image could save time, reduce noise, or both.

Motion of the subject may cause two types of image artifact in the current methods. First, motion will cause misregistration between the two image acquisitions, resulting in subtraction artifacts. Second, each image is liable to contain classic MR image "motion artifact": data aliasing in the phase-encoded y-coordinate caused by motion during each individual acquisition. These effects are particularly pernicious in the current setting because the signal of the interfering tissue is many times the blood signal that we wish to detect. Respiratory motion causes surprisingly little image artifact when imaging of the chest is performed in a coronal plane, perhaps because the motion in this case is predominantly along the z-coordinate, which is hidden. Bowel motion causes significant artifact in the current technique.

Since this work was prepared, a variation of imaging technique was found to provide a drastic reduction of motional artifacts. Systolic and diastolic images can be acquired concurrently by taking data for each image on alternating pulses; two such acquisitions are said to be "interleaved." By this means, image misregistration does not occur, and furthermore, the images have intrinsic motion artifacts that are nearly identical and cancel with subtraction, just like the background. Nonimaging 90° RF pulses must be inserted to equalize the repetition times of the two acquisitions, so that they will have equivalent T1 contrast.

Several studies have already indicated the usefulness of MR in the assessment of the vascular tree (11-17). This work extends these earlier methods. By exploiting flow-phase contrast, MR arteriograms have been obtained in the projective imaging format. These results are encouraging, but as we have indicated, the current method will not be the last word in MR angiography. Nevertheless, opinion is shifting in favor of the position that sensitive, reliable, and practical arteriography with MR imaging is possible. ∎

Send correspondence and reprint requests to: Van J. Wedeen, M.D., NMR Facility, Baker 2, Massachusetts General Hospital, 32 Fruit Street, Boston, MA 02114.

References
1. Zagzebski JA, Madsen EL. Physics and instrumentation in Doppler and B-mode ultrasonography. In: Zwiebel WJ, ed. Introduction to vascular ultrasonography. New York: Grune & Stratton, 1982; 1-21.
2. Lang EK. Prevention and treatment of complications following arteriography. Radiology 1967; 88:950-956.
3. Hahn EL. Spin echoes. Phys Rev 1950; 80(4):580-594.
4. Carr HY, Purcell EM. Effect of diffusion on free precession in nuclear magnetic resonance experiments. Phys Rev 1954; 94:630-638.
5. Singer JR, Crooks LE. Nuclear magnetic resonance blood flow measurements in the human brain. Science 1983; 221:654-656.
6. Wedeen VJ, Rosen BR, Chesler D, Brady TJ. MR velocity imaging by phase display. J Comput Assist Tomogr 1985; 9(3):530-536.
7. Wedeen VJ, Rosen BR, Buxton R, Brady TJ. Projective MRI angiography and quantitative flow-volume densitometry. Magn Reson Med (in press).
8. Moran PR, Moran RA, Karstaedt N. Verification and evaluation of internal flow and motion. Radiology 1985; 154:433-441.
9. Axel L. Blood flow effects in magnetic resonance imaging. AJR 1984; 143:1157-1166.
10. Wedeen VJ, Meuli RA, Edelman RR, et al. Projective imaging of pulsatile flow with magnetic resonance. Science 1985; 230:946-948.
11. Wesby GE, Higgins CB, Amparo EG, Hale JD, Kaufman L, Pogany AC. Peripheral vascular disease: correlation of MR imaging and angiography. Radiology 1985; 156:733-739.
12. Amparo EG, Hoddick WK, Hricak H, et al. Comparison of magnetic resonance imaging and ultrasonography in the evaluation of abdominal aortic aneurysms. Radiology 1985; 154:451-456.
13. Justich E, Amparo EG, Hricak H, Higgins CB. Infected aortoiliofemoral grafts: magnetic resonance imaging. Radiology 1985; 154:133-136.
14. Lee JKT, Ling D, Heiken JP, et al. Magnetic resonance imaging of abdominal aortic aneurysms. AJR 1984; 143:1197-1202.
15. Amparo EG, Higgins CB, Hoddick W, et al. Magnetic resonance imaging of aortic disease. AJR 1984; 143:1203-1209.
16. Herfkens RJ, Higgins CB, Hricak H, et al. Nuclear magnetic resonance imaging of arteriosclerotic disease. Radiology 1983; 148:161-166.
17. Glazer HS, Gutierrez FR, Levitt RG, Lee JKT, Murphy WA. The thoracic aorta studied by MR imaging. Radiology 1985; 157:149-155.
18. Hale JD, Valk PE, Watts JC, et al. MR imaging of blood vessels using three-dimensional reconstruction: methodology. Radiology 1985; 157:727-733.
19. Macovski A. Selective projection imaging: applications to radiology and NMR. IEEE Trans Med Imaging 1982; 1(1):42-47.
20. Meuli RA, Marquis C, Meister J-J, Mosimann R. Polytetrafluoroethylene grafts hemodynamics: a quantitative pulsed Doppler study (forthcoming).
21. Goslin RD, King DH. Processing arterial Doppler signals for clinical data. In: de Vilieger M, ed. Handbook of clinical ultrasound. New York: Wiley & Sons, 1978; 613-646.
22. Waluch V, Bradley WG. NMR even echo rephasing in slow laminar flow. J Comput Assist Tomogr 1984; 8(4):594-598.
23. Ehman RL, Felmlee JP, Julsrud PR, Gray JE. Vascular misregistration: a helpful sign in clinical MR imaging for characterizing blood flow in the plane of section (abstr.). Radiology 1985; 157(P):121.